ANALYSIS OF AIDING AND OPPOSING MIXED COVECTION IN VERTICAL SEMICIRCULAR DUCTS

A. A. Busedra

Mech. Eng. Dept., University of Garyounis, Benghazi, Libya
E-mail: kbusedra@garyounis.edu

الملخص

تم بحث الحمل المختلط للإنسياب الرقائقى المكتمل النمو عند تدفق المائع إلى أعلى وإلى أسفل في أنابيب رأسية نصف دائرية وللحصول على الحلول عددياً تم إستعمال طريقة (Finite–control volume approach) وذلك بإستخدام المعادلات الحاكمة وتم الحصول على النتائج بتطبيق حالتين: حرارة منتظمة محوريا مع درجة حرارة جدار منتظمة محيطياً (H1) وحرارة منتظمة محورياً ومحيطياً (H2). هذه النتائج تحتوي على السرعات والحرارة وقيم لمعامل الإحتكاك ورقم *Nusselt*. وجد أنه أثناء تدفق المائع إلى أعلى وإلى أسفل فإن توزيع السرعات ودرجات الحرارة يختلف عن الحمل القسري نتيجة لتأثير الحمل الحر. أما عند قيمة عالية لرقم *Grashof* فإن تركيز الخطوط الكونتورية للسرعات بالقرب من جدار الأنبوب للحالتين H1 و H2 يؤدي إلى زيادة في اجهاد القص. إضافة إلى ذلك فإن التركيز العالي للخطوط الكونتورية لدرجات الحرارة بالقرب من جدار الأنبوب أوضح تدرج عالي لدرجات الحرارة. ووجد أن الخطوط الكونتورية للسرعات بالقرب من جدار الأنبوب للحالة H2 أكثر تركيزا بقليل من الحالة H1 مما أدي إلى زيادة بسيطة في اجهاد القص. ونظراً لإختفاء الطبقات الحرارية عند قيم *Gr* العالية لوحظ أنه عند تدفق المائع إلى أعلى فإن $(fRe)_{H2}$ تزداد عن $(fRe)_{H1}$ وتنعكس عندما تكون $Nu_{H1} > Nu_{H2}$ عند أى قيمة لرقم *Grashof* بينما في حالة تدفق المائع إلى أسفل فان قيم معامل الاحتكاك وقيم *Nusselt* تقل بزيادة *Gr* للحالتين H1 و H2.

ABSTRACT

Laminar fully developed mixed convection in vertical semicircular ducts with upward and downward flows is investigated. Numerical solutions, obtained by using a control volume based finite difference approach, are presented for solving the governing equations. Results are obtained for the two limiting thermal boundary conditions; uniform heat input axially with uniform peripheral wall temperature (H1) and uniform heat input axially with uniform wall heat flux circumferentially (H2). These results include the velocity and temperature fields and data for the friction factor and Nusselt number. In aiding and opposing flows, the velocity and temperature distributions, due to the free convection effect, become different from the one corresponding to pure forced convection. At high *Gr*, the concentration of the isovel contours near the duct wall, for both thermal boundary conditions, leads to increased wall shear. In addition, the high concentration of isotherms near the wall shows high temperature gradient. The isovels for H2 are found to be slightly more concentrated near the wall which resulted in a slight increase in the wall shear as compared with the H1case. Due to the disappearance of the thermal stratification in H2 at higher values of *Gr*, it is noted that, when aiding the flow upward, $(fRe)_{H2}$ exceeds $(fRe)_{H1}$, and it reverses with $Nu_{H1} > Nu_{H2}$, for any value of *Gr*. However, when the flow is downward, the values of the friction factor and Nussult number decrease as *Gr* increases for both H1 and H2 thermal boundary conditions

.

KEYWORDS Vertical semicircular ducts; Laminar; Mixed convection; Heat flux.

INTRODUCTION

Semicircular ducts can be used to design compact heat exchangers and the flat wall of the semicircular duct can be attached on a nuclear reactor surface from which substantial heat might be released. The size of the literature dealing with laminar fully developed mixed convection in semicircular ducts is very sparse in comparison with vertical ducts of various cross sections, such as circular tubes [1-3] and parallel plates [4-6]. Other results for laminar fully developed mixed convection are available for rectangular ducts [7,8], triangular and rhombic ducts [9,10], elliptical ducts [11], and concentric annuli [12]. Most studies considered only upward flow with heating or downward flow with cooling. For this situation, the axial velocity profile is distorted from the parabolic shape to increase near the duct walls and decreases in the core, with the possibility of flow reversal in the core region at high Gr/Re ratio. Also the temperature field develops faster and heat transfer is enhanced with increasing Gr/Re ratio. The occurrence of reversed flow in the fully developed region for a particular geometry was also found to be strongly dependent on the thermal boundary condition imposed at the duct walls [6]. It should be noted that, in this study, no computations were made beyond the onset of flow reversal. For semicircular ducts the laminar forced convection in the entrance region has been studied by [13] and the fully developed region in circular sector ducts has been solved analytically by [14-16] with different thermal boundary conditions. These studies considered only forced convection without buoyancy effect. A few papers can be found in the literature dealing with mixed convection in semicircular ducts. Nandakumar et al. [17] studied numerically the problem of the fully developed mixed convection with the H1 thermal boundary condition in horizontal semicircular ducts with the flat wall at the bottom. Their numerical model produced dual solutions with two and four vortices in the secondary flow pattern. Lei and Trupp [18] solved the same problem considered in [17] using the H1 boundary condition but with the flat wall on top. Chinporncharoenpong et al. [19] studied the laminar fully developed mixed convection with the H1 thermal boundary condition in a horizontal semicircular duct. They presented results for the effects of orientation of the flat surface of horizontal semicircular ducts (from 0^o to 180^o with an incremental angle of 45^o) Chinporncharoenpong et al. [20] extended their study to horizontal circular sector ducts. They reported that the orientation effects are significant for the circular sector ducts only at high *Gr*. Busedra and Soliman [21] presented numerical results for laminar fully developed mixed convection in inclined semicircular ducts under buoyancy-assisted and buoyancy opposed conditions, using two boundary conditions H1 and H2. They noted that, thermal stratification in H2 was found to decrease in upward inclinations by increasing *Gr*. On the other hand, increasing *Gr* for downward inclinations appears to intensify thermal stratification. They also concluded that, as Gr increases, both Nusselt numbers for H1 and H2 develop a trend whereby their value increases with inclination angle up to a maximum and then decrease with further increase in the inclination angle. Other results for laminar mixed convection were obtained experimentally in the entrance region of a horizontal semicircular duct [22] and in the inclined semicircular duct [23]. Dong and Ebadian [24] studied the problem of fully developed mixed convection during laminar flow in a vertical semicircular duct with radial internal longitudinal fins. They presented some results for the friction factor and Nusselt number for upward flow of the finless semicircular duct and compared with those of finned semicircular ducts. However, no results currently exist for the velocity and temperature fields in vertical semicircular ducts, particularly in downward flow.

The objective of the present investigation is to generate theoretical results for laminar, fully developed mixed convection in vertical heated semicircular ducts with upward and downward flows. Two thermal boundary conditions will be used: uniform heat input axially with uniform peripheral wall temperature (known as the H1 boundary condition [25]), and uniform heat input axially with uniform wall heat flux circumferentially (the H2 boundary condition). The importance in the present study will be sited on the effects of free convection and thermal boundary condition on velocity and temperature fields, as well as the friction factor and Nussult number.

NUMERICAL ANALYSIS

Consider a vertical semicircular duct as shown in Figure (1). The fluid is characterized by steady laminar incompressible and fully developed hydrodynamically and thermally. Viscous dissipation is assumed to be negligible.

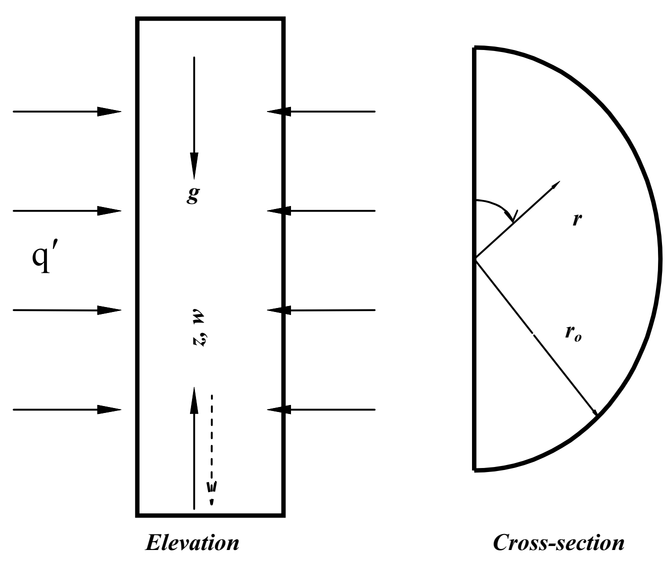

Figure 1: Geometry of the semicircular duct

Fluid properties are assumed to be constant, except for the density in the buoyancy terms which varies with the temperature according to Boussinesq approximation. Heat input is assumed to be uniform axially and two thermal boundary conditions, H1 and H2 are considered in this study.

Governing Equations

Momentum equation:

$$-\frac{\partial P}{\partial Z}+\frac{1}{R}\frac{\partial}{\partial R}\left(R\frac{\partial W}{\partial R}\right)+\frac{1}{R^2}\frac{\partial^2 W}{\partial \theta^2}+2\left(\frac{\pi}{\pi+2}\right)\left(\frac{Gr}{\mathrm{Re}}\right)\ T=0 \tag{1}$$

Energy Equation:

$$\frac{1}{R}\frac{\partial}{\partial R}\left(R\frac{\partial T}{\partial R}\right)+\frac{1}{R^2}\frac{\partial^2 T}{\partial \theta^2}\ =\ \left(\frac{2}{\pi}\right)\ W \tag{2}$$

where the dimensionless parameters and variables are:

$$R=\frac{r}{r_o}\ ,\ Z=\frac{z}{r_o}\ ,\ W=\frac{w}{w_m}\ ,\ D_h=\left(\frac{2\pi}{(2+\pi)}\right)\ r_0 \tag{3a}$$

$$T=\frac{t-t_r}{q'/k}\ ,\ \mathrm{Re}=\frac{D_h w_m}{\nu}\ ,\ Gr=\frac{g\beta q' r_o^3}{k\nu^2} \tag{3b}$$

The parameter t_r used in equation (3b) was taken t_w in the H1 boundary condition and $\bar{t}_w$ in the H2 boundary condition, while the term dP/dZ in equation (1) was treated as a constant (a consequence of the fully developed condition). The applicable boundary conditions are:

W = 0	on all walls	(4a)
T = 0	on all walls for the H1 condition	(4b)
$\frac{\partial T}{\partial R}=\frac{1}{\pi+2}$	at R = 1 for the H2 condition	(4c)
$\frac{\partial T}{\partial \theta}=-\frac{R}{\pi+2}$	at θ = 0 for the H2 condition	(4d)
$\frac{\partial T}{\partial \theta}=\frac{R}{\pi+2}$	at θ = π for the H2 condition	(4e)

Two important parameters used in engineering design are *Nu*, given by

$$Nu=\frac{hD_h}{k}=-\frac{2\pi}{(\pi+2)^2}\frac{1}{T_b} \tag{5}$$

and the product *fRe* , where the friction factor *f is* defined by

$$f = \frac{\overline{\tau}_w}{(1/2)\rho w_m^2} \tag{6}$$

The average wall shear stress, $\overline{\tau}_w$, was obtained by averaging the wall shear stress around the circumference of the duct and *fRe* is expressed in dimensionless form as:

$$f\,\mathrm{Re} = \frac{4\pi}{(\pi+2)^2}\left[\int_0^1\left(\frac{\partial W}{R\partial\theta}\right)_{\theta=0} dR - \int_0^1\left(\frac{\partial W}{R\partial\theta}\right)_{\theta=\pi} dR - \int_0^{\pi}\left(\frac{\partial W}{\partial R}\right)_{R=1} d\theta\right] \tag{7}$$

SOLUTION PROCEDURE

The dimensionless governing partial differential equations for fully developed flow and heat transfer were discretized by using a control volume based finite difference method [26]. A staggered grid was used in the computations with uniform subdivisions in the R and θ directions. The control volumes adjacent to the flat and curved walls were subdivided into two control volumes in order to capture the steep gradients in the temperature and velocity to ensure obtaining accurate values of the wall shear stress. For given values of the input parameters *Re* and *Gr*, computations started from an initial guess of the fields (*W, T,* and dP/dZ). The discretized equations were solved simultaneously for each radial line using the tridiagonal matrix algorithm [TDMA], and the domain was covered by sweeping line by line in the angular direction. At the end of each iteration, a correction procedure was applied to values of *W* and dP/dZ, using the conservation of mass, equation (8), in order to ensure that the mean value of the dimensionless velocity, W_m is equal to 1. This correction procedure follows the method outlined by Patankar and Spalding [27]. Thus the converged velocity profile must satisfy the following condition:

$$\int_0^{\pi}\int_0^{1} \mathrm{W R dR d\theta} = \frac{\pi}{2} \tag{8}$$

Iteration continued until the velocity and the temperature at all grid points as well as the value of dP/dZ satisfied the following convergence criterion.

$$\left|\frac{\phi_{new} - \phi_{old}}{\phi_{new}}\right| \le 10^{-6} \tag{9}$$

where ϕ is a scalar function.

VALIDATION OF NUMERICAL RESULTS

Numerical experimentation was conducted in order to determine the appropriate grid size. Different grid sizes for pure forced convection were used and the selected grid size of 30×48 $(R \times \theta)$ for smooth semicircular ducts is found to be capable of producing $(fRe)_o = 15.75$, $(Nu_{H1})_o = 4.086$, and $(Nu_{H2})_o = 2.926$. These values are within 0.13%, 0.073%, and 0.1%, respectively from the exact solution reported in [28]. The details of grid size effects and related numerical experimentations are delineated in [21]. For buoyancy assisted mixed convection in the vertical semicircular ducts, a comparison with the results in [24] is shown in Table (1). For the whole range of *Gr* covered in [24], the sets of results in Table (1) agree to within 0.5% in dP/dZ and to within 0.7% in Nu_{H1}.

Table 1: Comparison between the present results and those of Dong and Ebadian [24]

Gr	$-dP/dZ$		Nu_{H1}	
	Present	Ref [24]	Present	Ref [24]
0	21.09	21.11	4.086	4.088
6.4×10^4	29.97	30.00	4.313	4.314
6.4×10^5	95.96	96.16	5.795	5.780
3.2×10^6	296.4	297.9	8.831	8.772

RESULTS AND DISCUSSION

Numerical solutions were presented for upward and downward flows using the H1 and H2 thermal boundary conditions. The range of the governing parameters used in this study is $Re = 500$ and *Gr* up to 2×10^6. Numerical calculations were carried out for each thermal boundary condition with increasing values of *Gr* until flow reversal was detected. The detailed results for the distributions of the velocity and temperature followed by the behavior of the overall quantities *fRe* and *Nu* are discussed further below.

VELOCITY AND TEMPERATURE DISTRIBUTIONS

Under the effects of free convection, in case of vertical orientations in upward and downward flows, the velocity and temperature distributions become different from the one corresponding to pure forced convection ($Gr = 0$). Figure (2a) shows the isotherms and isovels at $Gr = 1 \times 10^5$ for the H1 case. The temperature and velocity contours are similar to the ones corresponding to pure forced flow, where the location of the maximum velocity and minimum temperature is confined to the horizontal radius ($\theta = \pi/2$). On the other hand, at the same *Gr* (shown in Figure (3a)), temperature stratification occupies the upper and lower parts of the cross-section in the H2 boundary condition and the isovels indicate high velocity gradients near the duct walls. However, the position of the maximum velocity and minimum temperature is still confined to the horizontal radius.

At $Gr = 2 \times 10^6$ the isovels and isotherms for H1 and H2 get considerably distorted, as show in figures (2b) and (3b). The area enclosed by the velocity contour at the top corner of the duct for H1 (Figure (2b)) and the smaller one for H2 (Figure (3b)) are high velocity contours. It can be seen that, the temperature stratification in H2 (Figure (3b)) is considerably reduced indicating much less circumferential variation in the wall temperature. The concentration of the isotherms and isovels near the duct wall, for both H1 and H2, leads to increased heat transfer and wall shear respectively. These concentrations of the isotherms and isovels near the duct wall are consistent with [11].

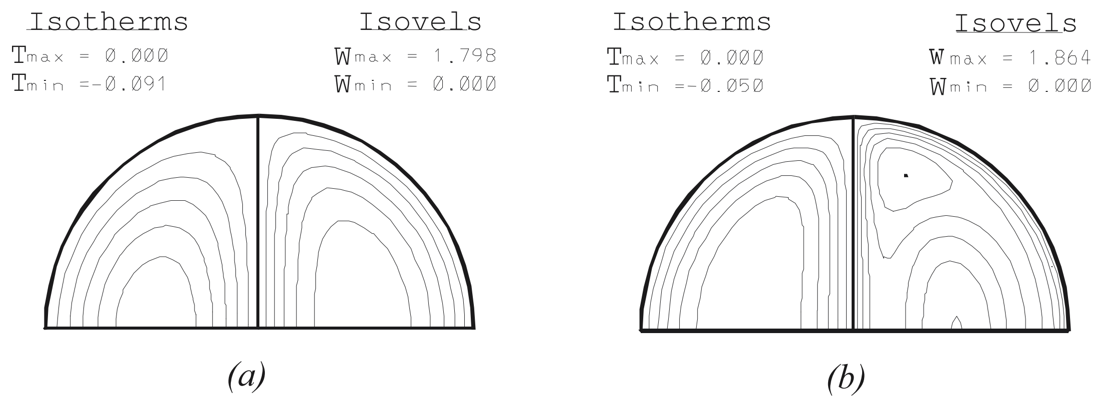

Figure 2: Velocity and temperature contours for H1 with aiding flow; (a) $Gr = 1 \times 10^5$ and (b) $Gr = 2 \times 10^6$

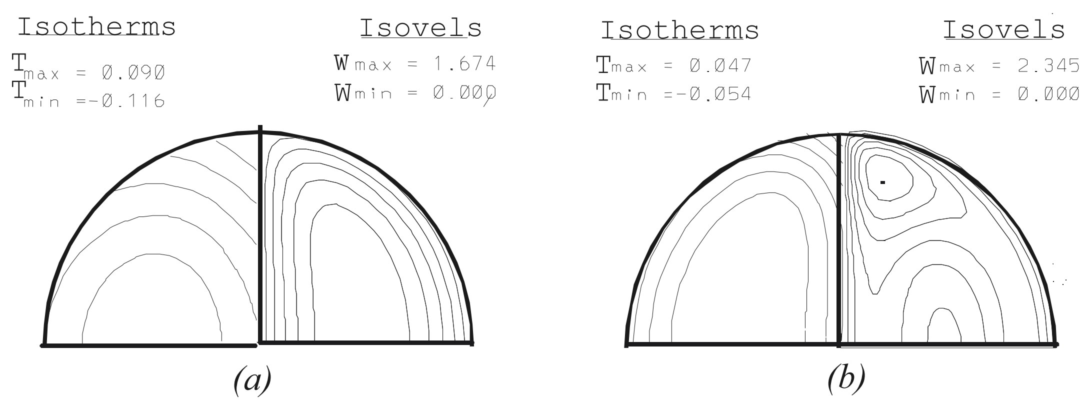

Figure 3: Velocity and temperature contours for H2 with aiding flow; (a) $Gr = 1 \times 10^5$ and (b) $Gr = 2 \times 10^6$

With downward flow, the maximum velocity and minimum temperature are located at the horizontal radius ($\theta = \pi/2$) of the cross-section, as shown in Figures (4) and (5). For the H2 thermal boundary condition, temperature stratification still occupied the upper and lower parts of the cross-section. Figures (4a) and (5a) for H1 and H2, respectively, show the velocity and temperature contours for $Gr = 1 \times 10^4$. The isovels and isotherms in these figures are nearly the same as the ones for pure forced convection. With increasing Gr, it can be seen in both thermal boundary conditions that the maximum velocity increases in magnitude but is still confined to the center. The difference in temperature (between T_{max} and T_{min}) is also increased, as shown in Figures

(4b) and (5b). Consequently, *fRe* and *Nu* for both thermal boundary conditions are expected to be lower than those for pure forced convection, as shown later.

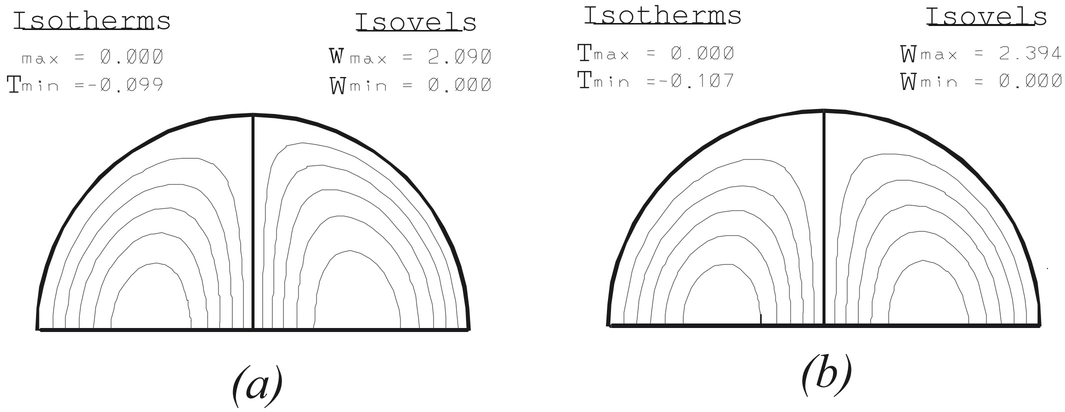

Figure 4: Velocity and temperature contours for H1 with opposing flow; (a) $Gr = 1 \times 10^4$ and (b) $Gr = 1 \times 10^5$

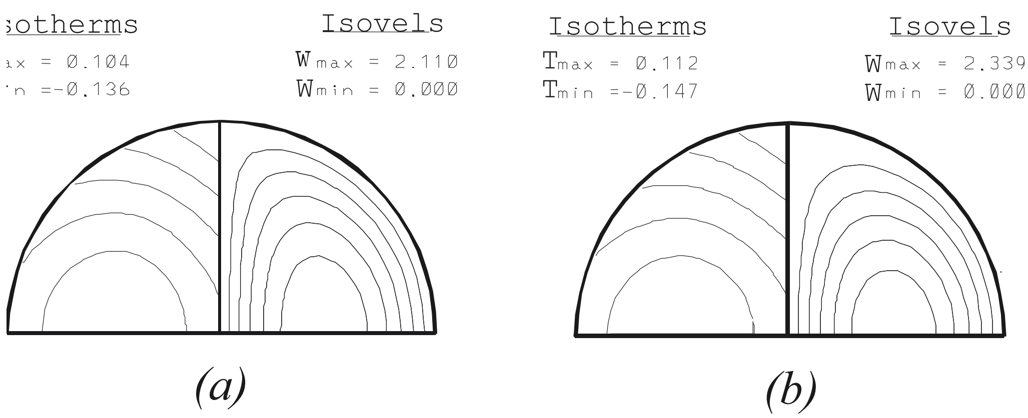

Figure 5: Velocity and temperature contours for H2 with opposing flow; (a) $Gr = 1 \times 10^4$ and (b) $Gr = 5 \times 10^4$

FRICTION FACTOR AND NUSSELT NUMBER

Due to the free convection, the friction factor and Nusselt number for buoyancy assisted mixed convection laminar flow are found to be substantially higher than those of pure forced convection, while for buoyancy opposed flow, the friction factor and Nusselt number were found to be lower than those of pure forced convection, as discussed in the following sections.

FRICTION FACTOR

Figure (8) shows the friction factor for upward and downward flows. The general trend in the results is that *fRe* increases with *Gr* for buoyancy assisted flow and decrease with *Gr* for buoyancy opposed flow for both thermal boundary conditions. For upward flow, the magnitude of this increase becomes larger as *Gr* increases. The effect of the thermal boundary condition is fairly small. As we can see that, $(fRe)_{H2}$ exceeds $(fRe)_{H1}$ due to the disappearance of the thermal stratification in H2.

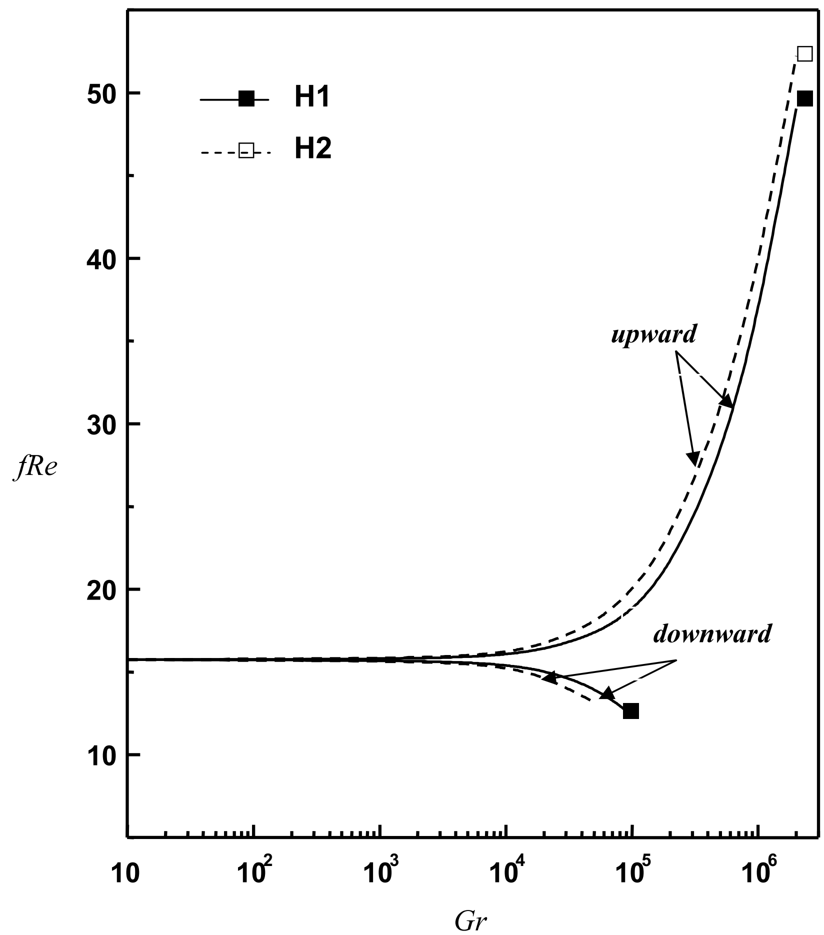

Figure 8: Friction factor results for upward and downward flows

NUSSELT NUMBER

The results for Nusselt number in upward and downward flows are presented in Figure (9). For upward flow it can be seen from these results that Nu_{H1} is always lager than Nu_{H2} for any value of *Gr*. At high *Gr* (e.g., $Gr \geq 1 \times 10^6$), we note that $Nu_{H1} > Nu_{H2}$ is still valid but with a slight difference between them. This is mainly due to the disappearance of the thermal stratification with increasing *Gr*. On the other hand, for downward flow, the trend is similar for the H1 and H2 thermal boundary conditions while Nu_{H1} is always higher than Nu_{H2} for any value of *Gr*.

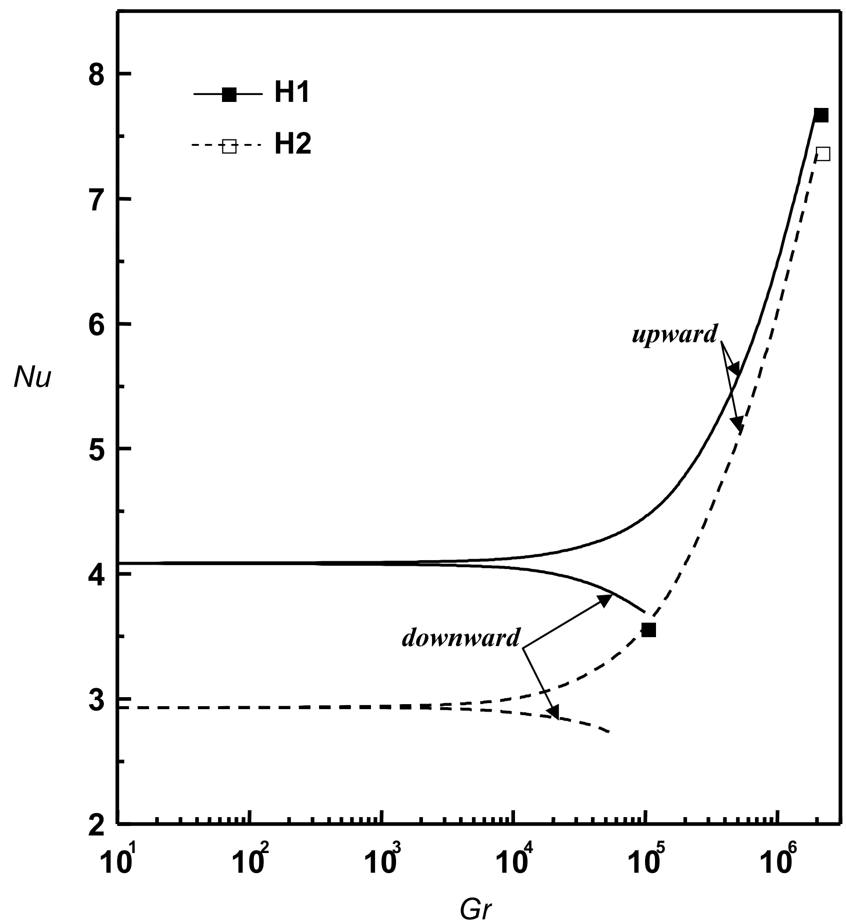

Figure 9: Nusselt number results for upward and downward flows

CONCLUSIONS

Numerical investigations were performed to analyze the problem of laminar fully developed mixed convection in vertical semicircular ducts with upward and downward flows. Two thermal boundary conditions were used: uniform heat input axially with uniform peripheral wall temperature (H1), and uniform heat input axially with uniform wall heat flux circumferentially (H2). Results for the velocity, temperature, friction factor, and Nusselt number were obtained for *Re* = 500 and a wide range of Grshof number. Therefore, one can conclude the following:

- In upward and downward flows, the velocity and temperature distributions, due to the free convection effect, become different from the one corresponding to pure forced convection. At high Gr, the concentration of the isovel curves near the duct wall, for both thermal boundary conditions, leads to increased wall shear. In the maen time, the high concentration of isotherms near the wall shows high temperature gradient. The isovels for H2 are found to be slightly more concentrated near the wall which resulted in a slight increase in the wall shear as compared whith the H1.

- *fRe* increases with *Gr* for buoyancy assisted flow and decreases with *Gr* for buoyancy opposed flow for both thermal boundary conditions. For upward flow, the magnitude of this increase becomes larger as *Gr* increases, in which $(fRe)_{H2}$ exceeds $(fRe)_{H1}$ due to the disappearance of the thermal stratification in H2.
- *Nu* also increases with *Gr* for upward flow and decreases with *Gr* for downward flow for both H1 and H2. In addition, Nu_{H1} is always lager than Nu_{H2} for any value of *Gr*. The difference between them becomes small as *Gr* gets higher.

REFERENCES

[1] Hallman, T.M, Combined Forced and Free – Laminar Heat Transfer in Vertical Tubes With Uniform Internal Heat Generation, *ASME Transactions, 78, 1831-1841*, 1956.

[2] Morton, B. R, Laminar Convection in Uniformly Heated Vertical Pipes*, Journal of Fluid Mechanics*, 8, (1960), 227-240.

[3] Martin A. and J. Shadday, Combined Forced / Free Convection Through Vertical Tubes at High Grashof Numbers, *Proceedings of the 8th International Heat Transfer Conference*, 3, (1986), 1433-1437.

[4] Aung W. and G. Worku, Theory of Fully Developed, Combined Convection Including Flow Reversal, *Journal of Heat Transfer*, 108, (1986), 485-488.

[5] Cheng C. H., H. S. Kuo, and W. H. Huang, Flow Reversal and Heat Transfer of Fully Developed Mixed Convection in Vertical Channels, *Journal of Thermo physics Heat Transfer*, 4, (1990), 375-383.

[6] Habhci S. and S. Acharya, Laminar Mixed Convection in Symmetrically or Asymmetrically Heated Vertical Channel, *Numerical Heat Transfer, Part A*, 9, (1986), 605-618.

[7] Iqbal M. amd B. D. Aggarwala, Combined Free and Forced Convection Through Vertical Rectangular Channel With Unequal Heating From Sides, *Journal of Applied Mechanics*, 93, (1971), 829-833.

[8] Cheng C. H. and C. J. Weng, Flow of Combined Convection in a Vertical Rectangular Duct With Unequally Isothermal Walls, *International Communication Journal of Heat and Mass Transfer*, 18, (1991), 127-140.

[9] Aggarwala B. D. and M. Iqbal, On Limiting Nusselt Numbers From Membrane Analogy for Combined Free and Forced Convection Through Vertical Ducts, *International Journal of Heat and Mass Transfer*, 12, (1969), 737-748.

[10] Iqbal M., B. D. Aggarwala, and A. G. Fowler, Laminar Combined Free and Forced Convection in Vertical Non-Circular Ducts Under Uniform Heat Flux, *International Journal of Heat and Mass Transfer*, 12, (1969), 1123-1139.

[11] Velusamy K. and V. K. Garg, Laminar Mixed Convection in Vertical Elliptic Ducts, *International Journal of Heat Transfer*, 39, (1996), 745-752.

[12] Maitra D. and K. S. Raju, Combined Free and Forced Convection Laminar Heat Transfer in a Vertical Annulus, *Journal of Heat Transfer*, 97, (1975), 135-137.

[13] Manglik R. M. and A. E. Bergles, Laminar Flow Heat Transfer in a Semi-circular Tube with Uniform Wall Temperature, *International Journal of Heat and Mass Transfer*, 30, no. 3, (1988), 625-636.

[14] Trupp A. C. and A. C. Y. Lau, Fully Developed Laminar Heat Transfer in a Circular Sector Duct with Isothermal Walls, *Journal of Heat Transfer*, 106, (1984), 467-469.

[15] Lei Q. M. and A. C. Trupp, Further Analysis of Laminar Flow Heat Transfer in Circular Sector Ducts, *ASME Journal of Heat Transfer*, 111, (1989), 1088-1090.

[16] Lei Q. M. and A. C. Trupp, Forced Convection of Thermally Developed Laminar Flow in Circular Sector Ducts, *Journal of Heat Transfer*, 33, no. 8, (1990), 1675-1683.

[17] Nandakumar K., J. H. Masliyah, and H. S. Law, Bifurcation in Steady Laminar Mixed Convection Flow in Horizontal Ducts, *Journal of Fluid Mechanics*, 152, (1985), 145-161.

[18] Lei Q. M. and A. C. Trupp, Prediction of Laminar Mixed Convection in a Horizontal Semicircular Duct, *6th Miami International Symposium on Heat and Mass transfer*, 4, (Dec. 1990), 10-12.

[19] Chinporncharoenpong C., A. C. Trupp, and H. M. Soliman, Effect of Gravitational Force Orientation on Laminar Mixed Convection for a Horizontal Semicircular Duct, *Proceedings of the 3rd World Conference on Experimental Heat Transfer, fluid Mechanics and Thermodynamics*, 1, (1993), 815-822.

[20] Chinporncharoenpong C., A. C. Trupp, and H. M. Soliman, Laminar Mixed Convection in Horizontal Circular Sector Ducts, *Proceedings of the Tenth International Heat Transfer Conference*, 5, (1994), 447-452.

[21] Busedra A. A. and H. M. Soliman, Analysis of Laminar Mixed Convection in Inclined Semicircular ducts Under Buoyancy Assisted and Opposed Conditions, *Numerical Heat Transfer, Part A*, 36, (1999), 527-544.

[22] Lei Q. M. and A. C. Trupp, Experimental Study of Laminar Mixed Convection in the Enrance Region of a Horizontal Semicircular Duct, *International Journal of Heat and Mass Transfer*, 34, (1991), 2361-2372.

[23] Busedra A. A. and H. M. Soliman, Experimental Investigation of Laminar Mixed Convection in an Inclined Semicircular Duct , *International Journal of Heat and Mass Transfer*, 34 (7), (2000), 1103– 1111.

[24] Dong Z. F. and M. A. Ebadian, Analysis of Combined Natural and Forced Convection in Vertical Semicircular Ducts With Radial Internal Fins, *Numerical Heat Transfer, Part A*, 27, (1995), 359-372.

[25] Shah R. K. and A. L. London, *Laminar Flow Forced Convection in Ducts*, Academic Press, New York, (1978).

[26] Patankar S. V, *Numerical Heat Transfer and Fluid Flow*, McGraw-Hill, New York, (1980).

[27] Patankar S. V. and D. B. Spalding, A Calculation Procedure for Heat, Mass and Momentum Transfer in Three-Dimensional Parabolic Flows, *International Journal of Heat and Mass Transfer*, 15, (1972), 1787-1806.

[28] Sparrow E. M. and A. Haji-Sheikh, Flow and Heat Transfer in Ducts of Arbitrary Shape with Arbitrary Thermal Boundary Conditions, *Journal of Heat Transfer,* 88, (1966), 351-358.

NOMENOCLATURE

D_h	hydraulic diameter
f	friction factor
g	gravitational acceleration
Gr	Grashof number
h	average heat transfer coefficient
H1	uniform heat input axially with uniform peripheral wall temperature
H2	uniform heat input axially with uniform wall heat flux circumferentially
k	thermal conductivity
Nu	Nusselt number
P	dimensionless cross-sectional average pressure
q'	rate of heat input per unit length
r	radial coordinate
r_o	radius of circular wall
R	dimensionless radial coordinate
Re	Reynolds number
s	distance along the duct circumference
t	temperature
T	dimensionless temperature
w	axial velocity
W	dimensionless axial velocity
z	axial coordinate
Z	dimensionless axial coordinate
β	coefficient of thermal expansion
ϕ	scalar function
ν	kinematic viscosity
ρ	density
τ	wall shear stress

Subscripts

b	bulk value
$_{H1}$	corresponding to the H1 boundary condition
$_{H2}$	corresponding to the H2 boundary condition
m	mean
o	corresponding to $Gr = 0$
w	at the wall